

See discussions, stats, and author profiles for this publication at: <https://www.researchgate.net/publication/40849503>

# Density Functional Investigation of Structure and Stability of Ge- $n$ and Ge $n$ Ni ( $n=1-20$ ) Clusters: Validity of the Electron Counting Rule

ARTICLE *in* THE JOURNAL OF PHYSICAL CHEMISTRY A · FEBRUARY 2010

Impact Factor: 2.69 · DOI: 10.1021/jp905561n · Source: PubMed

---

CITATIONS

28

---

READS

22

## 2 AUTHORS:



[Debashis Bandyopadhyay](#)

Birla Institute of Technology and Science P...

49 PUBLICATIONS 239 CITATIONS

SEE PROFILE



[Prasenjit Sen](#)

Harish-Chandra Research Institute

61 PUBLICATIONS 675 CITATIONS

SEE PROFILE

# Density Functional Investigation of Structure and Stability of $\text{Ge}_n$ and $\text{Ge}_n\text{Ni}$ ( $n = 1-20$ ) Clusters: Validity of the Electron Counting Rule

Debashis Bandyopadhyay<sup>†</sup> and Prasenjit Sen<sup>\*,‡</sup>

Physics Group, Birla Institute of Technology and Science, Pilani - 333031, Rajasthan, India, and  
Harish-Chandra Research Institute, Chhatnag Road, Jhansi, Allahabad-211019, U.P, India

Received: June 14, 2009; Revised Manuscript Received: December 4, 2009

Structure and electronic properties of neutral and cationic pure and Ni-doped Ge clusters containing 1–20 Ge atoms are calculated within the framework of linear combination of atomic orbitals density functional theory. It is found that in clusters containing more than 8 Ge atoms the Ni atom is absorbed endohedrally in the Ge cage. Relative stability of Ni-doped clusters at different sizes is studied by calculating their binding energy, embedding energy of a Ni atom in a Ge cluster, highest-occupied molecular orbital to lowest-unoccupied molecular orbital gap, and the second-order energy difference. Clusters having 20 valence electrons turn out to be relatively more stable in both the neutral and the cationic series. There is, in fact, a sharp drop in IP as the valence electron count increases from 20 to 21, in agreement with predictions of shell models. Relevance of these results to the designing of Ge-based superatoms is discussed.

## 1. Introduction

Atomic clusters consisting of a few to a few hundred atoms have come to be accepted as a new “phase” of matter. Properties of such clusters sensitively depend on their size and composition. This throws up fundamental questions and opens up exciting possibilities of novel applications. Clusters of both (bulk) metallic and semiconductor elements have been studied extensively. In this age of nanotechnology, study of Si and Ge clusters has attracted a lot of theoretical and experimental attention due to their importance in the electronic industry.<sup>1–17</sup> However, both pure Si and Ge clusters are chemically reactive.<sup>18</sup> Therefore one needs to stabilize them for any potential application. Two ways of enhancing stability of Si clusters have been identified: the first involves encapsulating a metal atom inside a Si cage. Transition metal (TM)-doped Si cage clusters have attracted particular attention.<sup>19–21</sup> Such clusters exhibit many novel behaviors because the TM atom can saturate the dangling bonds on the Si atoms.<sup>22,23</sup> The second way is to attach hydrogen atoms exohedrally. It has been found that the fullerene-like hydrogenated silicon cages  $\text{Si}_n\text{H}_n$  with  $n = 20, 28, 30, 36, 50$ , and  $60$  are very stable with large energy gaps suitable for optoelectronic and several other applications.<sup>16–28</sup> As for Ge clusters, along with hydrogenation,<sup>28</sup> forming zintl anions with or without TM atoms is also an effective way of stabilizing them.<sup>29,30</sup>

As compared to Si clusters, only a few theoretical contributions have been made by different groups on the endohedral doping of TM elements in pure as well as hydrogenated Ge cages.<sup>17,20</sup> Theoretical studies on TM-doped caged  $\text{Ge}_n\text{TM}$  ( $n = 14-16$ ) clusters<sup>17</sup> indicate that the growth behavior of these clusters are different from those of metal encapsulated silicon clusters. The highest-occupied molecular orbital to lowest-unoccupied molecular orbital (HOMO–LUMO) gaps in such clusters are much higher than their Si counterparts.

One question that has been widely debated in the context of  $\text{Si}_n\text{TM}$  clusters is whether their relative stability obeys 18-

electron rule (also known as the octet rule)<sup>31</sup> or other electron counting rules. The octet rule claims that when the total number of valence electrons on a TM atom surrounded by other atoms or ligands is 18 the molecule or ion is particularly stable. By assumption that each Si atom donates one valence electron to the encapsulated TM atom, the total valence electron count on the latter is  $n + n'$ , when  $n'$  is the number of valence electrons on the TM atom. By this argument,  $\text{Si}_{12}\text{Cr}$  and  $\text{Si}_{12}\text{W}$  (both with  $n' = 6$ ) should be the most stable clusters in the 3d and 5d TM-doped  $\text{Si}_{12}$  series, respectively. However, Sen and Mitas<sup>32</sup> and Guo et al.<sup>33</sup> in their calculations found  $\text{Si}_{12}\text{V}$  to be the most stable one in the 3d series, indicating that the octet rule may not always be valid. Reveles and Khanna<sup>34</sup> argued that (a) valence electrons in  $\text{Si}_n\text{TM}$  clusters can be described by a nearly free-electron gas, and (b) one needs to invoke the Wigner–Witmer (WW) spin conservation rule<sup>35</sup> while calculating embedding energies (EE). In the nearly free-electron gas picture the metal atom is assumed to donate all its valence electrons, and each Si atom is assumed to donate one electron to the valence pool. Then using the WW rule they showed that  $\text{Si}_{12}\text{Cr}$ , indeed, has the highest EE in the neutral 3d TM-doped  $\text{Si}_{12}$  series.<sup>34</sup>  $\text{Si}_{12}\text{Fe}$  has a smaller peak, which can be justified as originating from a 20-electron filled shell electronic configuration. Among the anionic clusters,  $\text{Si}_{12}\text{V}^-$  has the highest EE, being an 18-electron cluster. It is worth mentioning here that according to various shell models of the delocalized electrons in metal clusters, 2, 8, 18, and/or 20 are shell-filling numbers.<sup>36</sup> Metal clusters with 18 or 20 valence electrons are found to be more stable than others. Though TM–Si clusters seem unlikely to be describable by models of completely delocalized valence electrons, Reveles and Khanna<sup>34</sup> have shown that stability of some of them can be rationalized within a free-electron gas picture. However, the free-electron gas picture is not valid in every case. There is no peak in EE at  $\text{Si}_{12}\text{Mn}^-$ , which is a 20-electron cluster. Moreover, there is a small peak at  $\text{Si}_{12}\text{Co}^-$ , which is a 22-electron cluster. Thus, even the WW rule may not justify applicability of the electron counting rule in every case. On the other hand, experiments have supported the validity of these electron-counting rules in some cases. Koyasu et al.<sup>37</sup> studied the

\* To whom correspondence should be addressed. E-mail: prasen@hri.res.in.

<sup>†</sup> Birla Institute of Technology and Science.

<sup>‡</sup> Harish-Chandra Research Institute.

electronic and geometrical structures of  $\text{Si}_{16}\text{TM}$  (TM = Sc, Ti, and V) clusters by mass spectrometry and anion photoelectron spectroscopy. They found that neutral  $\text{Si}_{16}\text{Ti}$ , being a 20-electron cluster, had a closed-shell electron configuration with a large HOMO–LUMO gap. An offshoot of such electron counting rules is that  $\text{Si}_{16}\text{V}$ , which has one electron more than a closed-shell configuration, has a low IP. Thus, it mimics alkali atoms of the periodic table. Stable clusters that mimic chemical or other properties of atoms on the periodic table have been termed superatoms.<sup>38</sup> With a low IP, like alkali atoms,  $\text{Si}_{12}\text{V}$  forms an ionic complex with the halogen atom F.<sup>39</sup>

With this backdrop, we study properties of Ni-doped  $\text{Ge}_n$  clusters over the large size range  $n = 1$ –20. Geometry, electronic structure, growth behavior, and stability of neutral and cationic  $\text{Ge}_n\text{Ni}$  clusters are studied using density functional theory (DFT) methods. Although Ni-doped  $\text{Ge}_n$  clusters have been theoretically studied before,<sup>17</sup> these were limited to a smaller size range.  $\text{Ge}_{10}\text{Ni}$  was found to be the most stable cluster in the size range explored, but no attempt was made to rationalize that. Therefore, apart from studying their growth patterns, our main focus is to understand if relative stability of these clusters can be understood in terms of electron counting rules, as this would open up possibilities of designing Ge-based superatoms. As we discuss in detail below, clusters with 20 valence electrons turn out to be particularly stable in both neutral and cationic series.

The rest of the paper is organized as follows. In section 2 we discuss the computational methods used for these studies. In section 3 we present and discuss our results for structural and electronic properties of pure and Ni-doped Ge clusters.

## 2. Computational Methods

Self-consistent-field (SCF) electronic structure calculations were carried out on all clusters within the framework of Kohn–Sham DFT. Molecular orbitals (MO) are expressed as linear combination of atom-centered basis functions for which the LANL2DZ basis set and associated effective core potential (ECP) is used on all atoms. Spin-polarized calculations are carried out using the Becke three-parameter exchange and the Perdew–Wang generalized gradient approximation (GGA) (B3PW91) functionals.<sup>40–43</sup> For all clusters, geometries were optimized without any symmetry constraints starting from a number of initial configurations and for different spin states. Stability of the structures is checked by calculating their harmonic vibrational frequencies. If any imaginary frequency is found, a relaxation along that vibrational mode is carried out until the true local minimum is obtained. To check the validity of the applied theoretical methodologies, some test calculations were carried out on Ge–Ge dimer using the B3PW91/LANL2DZ (5D, 7F) combination. The predicted Ge–Ge bond length of 2.54 Å is comparable to 2.44 Å obtained using a multireference configuration interaction method.<sup>44</sup> Theoretical calculations are performed with Gaussian 98 and Gaussian 03 program packages.<sup>45</sup>

## 3. Results and Discussion

**A. Growth Pattern of Pure  $\text{Ge}_n$  Nanoclusters.** In this section we present our results for the structure of pure  $\text{Ge}_n$  ( $n = 1$ –20) clusters. Our focus is not on pure  $\text{Ge}_n$  clusters, and we will not discuss them in detail here. However, we still need to study them for the following reasons: (i) to benchmark our calculations against known results; (ii) to know the ground-state isomers and their total energies in order to calculate the EE (defined later) of a Ni atom in them.

The first member of the pure  $\text{Ge}_n$  series studied is  $\text{Ge}_2$ . A triplet spin state is found to be the ground state. This is consistent with results of Wang and Han.<sup>17</sup> Geometries of this and all other  $\text{Ge}_n$  clusters studied in this work are shown in Figure 1. We studied two geometries for the  $\text{Ge}_3$  cluster: a triangle and a linear chain. The  $\text{Ge}_3(\text{A})$  (isosceles triangle) structure (Figure 1) having  $C_{2v}$  point group symmetry turns out to be the ground state. Two structures are studied for the  $\text{Ge}_4$  cluster: a planar rhombus ( $D_{2h}$ ) and a tetrahedron ( $T_d$ ). The planar rhombus is found to be 2.15 eV lower in energy than the  $T_d$  structure. These are in general agreement with previous works.<sup>10,12,14</sup>

We find two stable structures for  $\text{Ge}_5$  clusters. The triangular bipyramid structure ( $D_{3h}$ ) is lower in energy by 0.41 eV compared to the distorted pentagonal structure shown in Figure 1. This is in agreement with the results of Archibong and St-Amant.<sup>10</sup> It is to be noted that Wang and Han<sup>17</sup> found the same structure as unstable with the presence of two imaginary frequencies. In the present calculations all frequencies of this structure are found to be real, and hence it is a stable ground-state cluster. A little modification over the ground-state structure of  $\text{Ge}_5$  gives the out-of-plane edge-capped  $\text{Ge}_6(\text{A})$  ground-state isomer with  $C_s$  symmetry. The other isomer,  $\text{Ge}_6(\text{B})$  with  $C_1$  symmetry, is nearly degenerate. Three different isomers are found for  $\text{Ge}_7$ . Out of these the pentagonal bipyramid  $\text{Ge}_7(\text{A})$  with  $D_{5h}$  symmetry is the ground state. The next stable structure  $\text{Ge}_7(\text{B})$  is a typical multirhombus structure composed of planar or bent rhombi and has  $C_s$  symmetry. The third isomer  $\text{Ge}_7(\text{C})$  is also a stable structure generated with one germanium atom being face capped on the top of the boatlike cluster with  $C_{3v}$  symmetry. These again are in general agreement with previous studies.<sup>10–14</sup>

As far as the  $\text{Ge}_8$  cluster is concerned, three different stable structures are found. The ground-state  $\text{Ge}_8(\text{A})$  structure is obtained by adding one germanium atom above the plane of the capped hexagonal structure of  $\text{Ge}_7(\text{A})$ .  $\text{Ge}_8(\text{A})$  is only marginally lower in energy than  $\text{Ge}_8(\text{C})$ , which is the capped pentagonal bipyramid as reported by Wang et al.<sup>11</sup> The energy difference is 0.08 eV. Wang et al. had found this capped pentagonal bipyramid structure to be the ground state. Previous FP-LMTO calculations also pointed out that the boatlike structure of  $\text{Ge}_8(\text{A})$  cluster with  $C_1$  symmetry is the most stable structure.<sup>46</sup>

Two different structures are found for  $\text{Ge}_9$  with  $\text{Ge}_9(\text{A})$  as the ground state, as shown in Figure 1. The total energy of  $\text{Ge}_9(\text{A})$  is very close to those of the other two isomers. In the present study, we find two stable isomers for  $\text{Ge}_{10}$ . The lowest energy structure  $\text{Ge}_{10}(\text{A})$  can be viewed as a tetracapped trigonal prism. Another stable, bucketlike isomer  $\text{Ge}_{10}(\text{B})$  can be described as a pentagonal prism with two irregular pentagons. Total energy of the first isomer is lower than the pentagonal prism structure by 1.38 eV. In  $\text{Ge}_{11}$ , the isomer  $\text{Ge}_{11}(\text{A})$  is the ground-state, and it can be obtained by capping a Ge atom at the top of the  $\text{Ge}_{10}(\text{A})$  cluster.  $\text{Ge}_{11}(\text{A})$  is, however, only 0.13 eV lower in energy than  $\text{Ge}_{11}(\text{B})$ .

Most of the structures for  $\text{Ge}_n$  for  $n$  (11–20) have been obtained by optimizing the structures of pure Si clusters of the same size as reported by Ho et al.<sup>1</sup> and Mitas et al.<sup>47</sup> after appropriately expanding the bond lengths. Almost identical geometries as those for  $\text{Si}_n$  clusters, with only small variations, are the ground states of pure Ge clusters also. The ground-state  $\text{Ge}_{12}(\text{A})$  is a combination of four rhombi and four pentagons and has  $C_1$  symmetry. This is 0.9 eV lower in energy than  $\text{Ge}_{12}(\text{B})$  also with  $C_1$  symmetry. The third structure  $\text{Ge}_{12}(\text{C})$  is

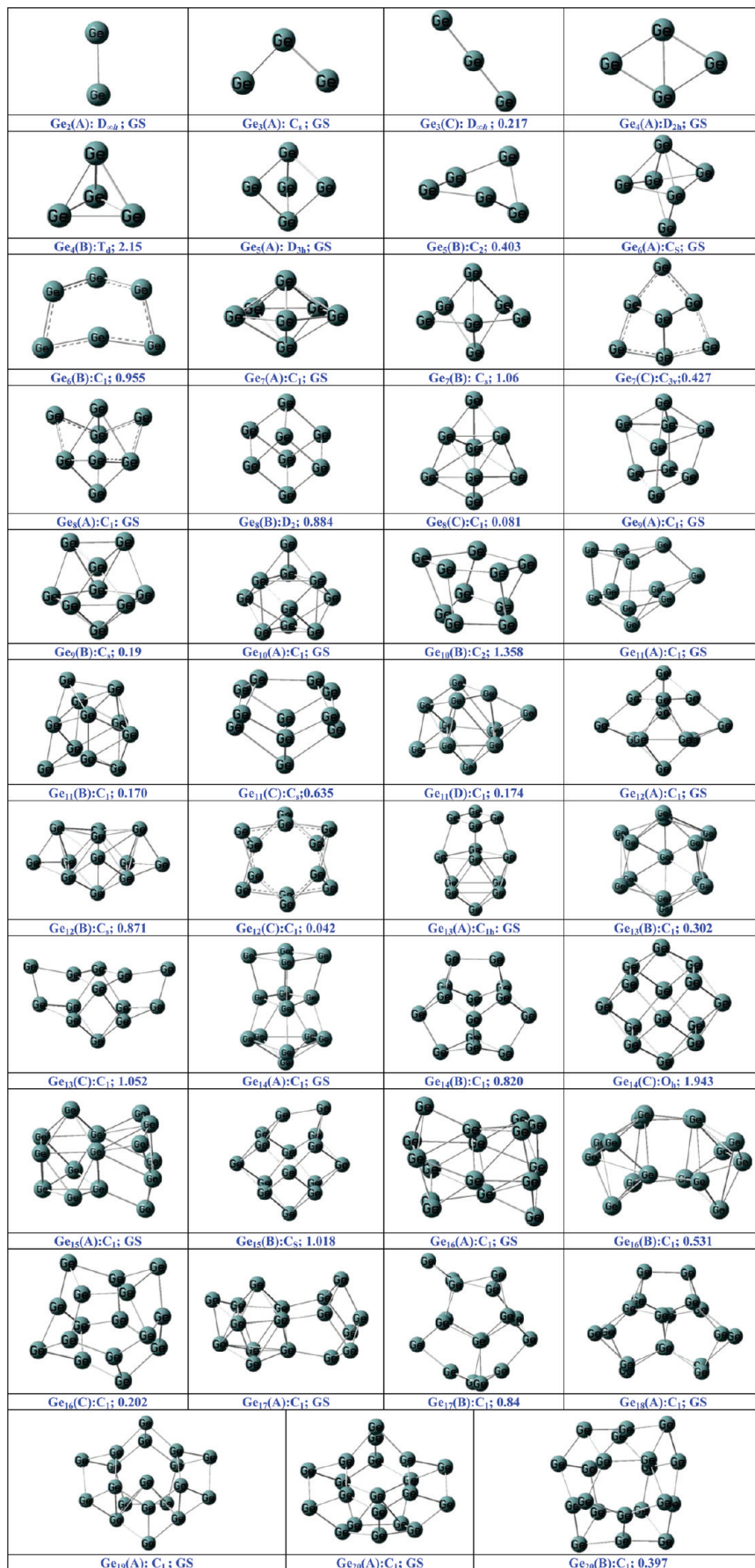


**Figure 1.** Optimized structures of pure Ge<sub>n</sub> clusters for *n* = 2–20 with the point group symmetry and relative energies (in electronvolts) with respect to the ground-state (GS) isomer in each size.



a combination of two parallel irregular hexagons and also has  $C_1$  point group symmetry.

For  $Ge_{13}$  clusters, the structure  $Ge_{13}(A)$  is the ground state and has the same symmetry as that of a  $Si_{13}$  cluster reported by Ho et al. Of the other two stable structures,  $Ge_{13}(B)$  is a basketlike structure, and  $Ge_{13}(C)$  is a bird's wings structure similar to  $Ge_{12}(B)$ .

For  $Ge_{14}$ , the ground-state isomer  $Ge_{14}(A)$  has the same  $C_1$  structure as obtained earlier for  $Si_{14}$ , except for the difference in bond lengths. In addition to this, two different cage structures are also obtained. The first one,  $Ge_{14}(B)$ , has a  $C_s$  symmetry. It has six pentagons and three rhombi with an optimized energy 1.12 eV lower than that of the isomer  $Ge_{14}(C)$ , which has  $O_h$  symmetry. The fact that the  $C_s$  isomer is lower in energy confirms that  $Ge_n$  clusters with pentagons and isolated rhombi are more favorable and follow the isolated rhombus rule<sup>48</sup> as carbon fullerenes.

$Ge_{15}$  has a ground-state structure,  $Ge_{15}(A)$ , similar to that of  $Si_{15}$ . Among the other cagelike structures,  $Ge_{15}(B)$  is quite similar to  $Ge_{14}(B)$ . The ground-state structure for  $Ge_{16}$ ,  $Ge_{16}(A)$ , is similar to the ground-state isomer of the  $Si_{16}$  as reported by Bandyopadhyay.<sup>49</sup> Pure cagelike germanium clusters with  $16 < n \leq 20$  are not symmetrical structures in the present study as shown in Figure 1. For all the above sizes, the structure reported by Ho et al. is found to be the ground state in germanium also (except for  $n = 17$ ) and are shown in Figure 1.

In the size range  $n = 9-18$  our lowest energy structures are slightly different from those reported by Wang et al.<sup>11</sup> and Wang et al.<sup>13</sup> The structures obtained previously<sup>11,13</sup> are generally more symmetric. Our structures for  $n = 19$  and 20, however, agree well with B3LYP/LANL2DZ results of Ma and Wang.<sup>15</sup>

**B. Growth Pattern of Hybrid  $Ge_nNi$  Clusters.** Now we discuss our results on Ni-doped Ge clusters. There are several reasons for which one would be interested in these clusters. As we discussed above for  $Ge_n$  clusters and found earlier for  $Si_n$  clusters, these elements do not form stable fullerene cages due to their unfavorable  $sp^2$  hybridization. However, encapsulating a TM atom can stabilize Si cages. The same is expected to be true of Ge cages as well. Also, recent studies<sup>50-54</sup> have shown that metal-doped cagelike isomers are important because of their novel properties that can be useful in varied applications. But our main focus is to understand if the relative stability of these clusters can be understood in terms any simple electron counting rule. This would be the first step in identifying the stable species, and the possible candidates for designing Ge-based superatoms.

Structure of a  $GeNi$  dimer is optimized for both singlet and triplet spin states. The singlet turns out to be the ground state with the triplet state being 0.98 eV higher in energy. Note that Wang and Han<sup>17</sup> had found the triplet state to be lower in energy. The cluster for  $n = 2$  is also optimized for singlet and triplet states. Three different optimized structures are found in this case. Among these three, the triangular structure  $Ge_2Ni(A)$  in the triplet spin state is the ground state. All the structures for  $Ge_nNi$  clusters studied here are shown in Figure 2. For the  $Ge_3Ni$  clusters, four stable optimized geometries are found. The rhombus structure in singlet spin state is the ground state. In fact, all larger Ni-doped clusters have singlet ground states. Our results for these clusters agree with those of Wang and Han.<sup>17</sup>

In the  $Ge_4Ni$  family, three different isomers are found with  $Ge_4Ni(A)$  being the ground state. This structure can be obtained by capping a Ni atom on a  $Ge_4$  rhombus. In the optimized structure the rhombus distorts by bending. Two different structures are obtained for  $Ge_5Ni$ . The ground-state  $Ge_5Ni(A)$  in this series has  $C_1$  point group symmetry. Three different

structures for  $Ge_6Ni$  are based on the structures  $Ge_6(A)$  and  $Ge_7(A)$  of pure Ge clusters. The optimized ground-state structure  $Ge_6Ni(A)$  is obtained by replacing one of the Ge atoms in  $Ge_6(A)$  by a nickel atom and adding one extra germanium atom on a triangular face. The other structures shown in Figure 2 can be obtained by replacing one germanium atom in  $Ge_7(A)$  from different positions. The ground-state structure  $Ge_7Ni(A)$  in  $n = 7$  series is similar to the ground-state structure obtained by Wang and Han.<sup>17</sup> Addition of a nickel atom to one of the faces of  $Ge_7(A)$  gives the structure  $Ge_7Ni(B)$  as shown in Figure 2. The third structure  $Ge_7Ni(C)$  is similar to the ground-state structure  $Ge_7Ni(A)$  except the position of Ni atom. All the three structure have  $C_1$  point group symmetry.

With increasing size of the clusters, their tendency to encapsulate a nickel atom increases. In  $Ge_8Ni(A)$  the nickel atom is enclosed by the Ge atoms except on one side. In an earlier work, Bandyopadhyay<sup>49</sup> found a similar structure for TM-doped silicon cluster of the same size. The smallest Ge cluster that can completely encapsulate a nickel atom is  $Ge_9$ . Guo et al.<sup>49</sup> have shown that the smallest metal-encapsulating cagelike structure for  $Si_nNi$  clusters is formed at  $n = 10$ . Probably it is the larger size of a  $Ge_n$  cage that allows such a structure at a smaller size. The ground-state in this series is  $Ge_9Ni(A)$  with  $C_1$  point group symmetry. There are six stable isomers in this series, three of which, (A), (B), and (D), have endohedral Ni atoms. There are two stable isomers for  $Ge_{10}Ni$ , both of which have endohedral Ni atoms. In fact, as already mentioned, for  $n > 8$  the ground state always has the Ni atom encapsulated by a Ge cage. The clusters  $Ge_{11}Ni(A)$  and  $Ge_{12}Ni(A)$ , both having  $C_1$  point group symmetry, are the ground-state isomers at these sizes. The structure  $Ge_{12}Ni(A)$  is a combination of four pentagons and four rhombi. This combination always gives better stability.<sup>55</sup> The Ni-encapsulated hexagonal prism  $Ge_{12}Ni(D)$  is a stable isomer but is not the ground state. Previous investigations on TM (Ti, Zr, and Hf)-encapsulated silicon clusters had found metal-encapsulated hexagonal prism to be the lowest-energy structure.<sup>49</sup> The ground state of the  $Ge_{12}Zn$  isomer was found to be a perfect icosahedron, and its total energy was lower than that of the hexagonal prism structure.<sup>55</sup> But for a Ni-doped  $Ge_{12}$  cluster, none of these happens to be the ground state. Among the  $Ge_{11}Ni$  clusters,  $Ge_{11}Ni(B)$  cannot absorb Ni atom endohedrally, but the  $Ge_{11}Ni(A)$  and all five structures of  $Ge_{12}Ni$  absorb the nickel endohedrally. This supports our claim that larger Ge clusters tend to encapsulate the Ni atom.

As for  $Ge_{13}Ni$ , two different stable structures are obtained. The ground-state  $Ge_{13}Ni(A)$  is a capped hexagonal structure with the Ni atom inside the cage. The second structure,  $Ge_{13}Ni(B)$ , is a combination of five rhombi and four pentagons symmetrically placed on the base rhombi. Though this is a combination of pentagons and rhombi, this is not the ground-state structure. This could be due to the existence of strain on the surface because four rhombi share a common vertex which is not the case in  $Ge_{12}Ni(A)$ . By adding one Ge atom to the common vertex of the four rhombi in  $Ge_{13}Ni(B)$ , one gets the ground-state structure  $Ge_{14}Ni(A)$  with  $C_1$  symmetry. In this structure there are six pentagons and three rhombi. Addition of one Ge atom converts two rhombi into two pentagons. The second optimized isomer in this series  $Ge_{14}Ni(B)$  is a symmetric hexagonal bicapped structure with a total of eight rhombi. The lower total energy of the  $Ge_{14}Ni(A)$  again confirms that structures with pentagons and isolated rhombi are more favorable and follow the isolated rhombus rule<sup>48</sup> as in carbon fullerenes.

The structure  $Ge_{15}Ni(A)$  is quite similar to that of  $Ge_{14}Ni(A)$ . It can be viewed as addition of one Ge atom to the bottom of the rhombi in  $Ge_{14}Ni(A)$ . The optimized  $Ge_{15}Ni(A)$  structure consists

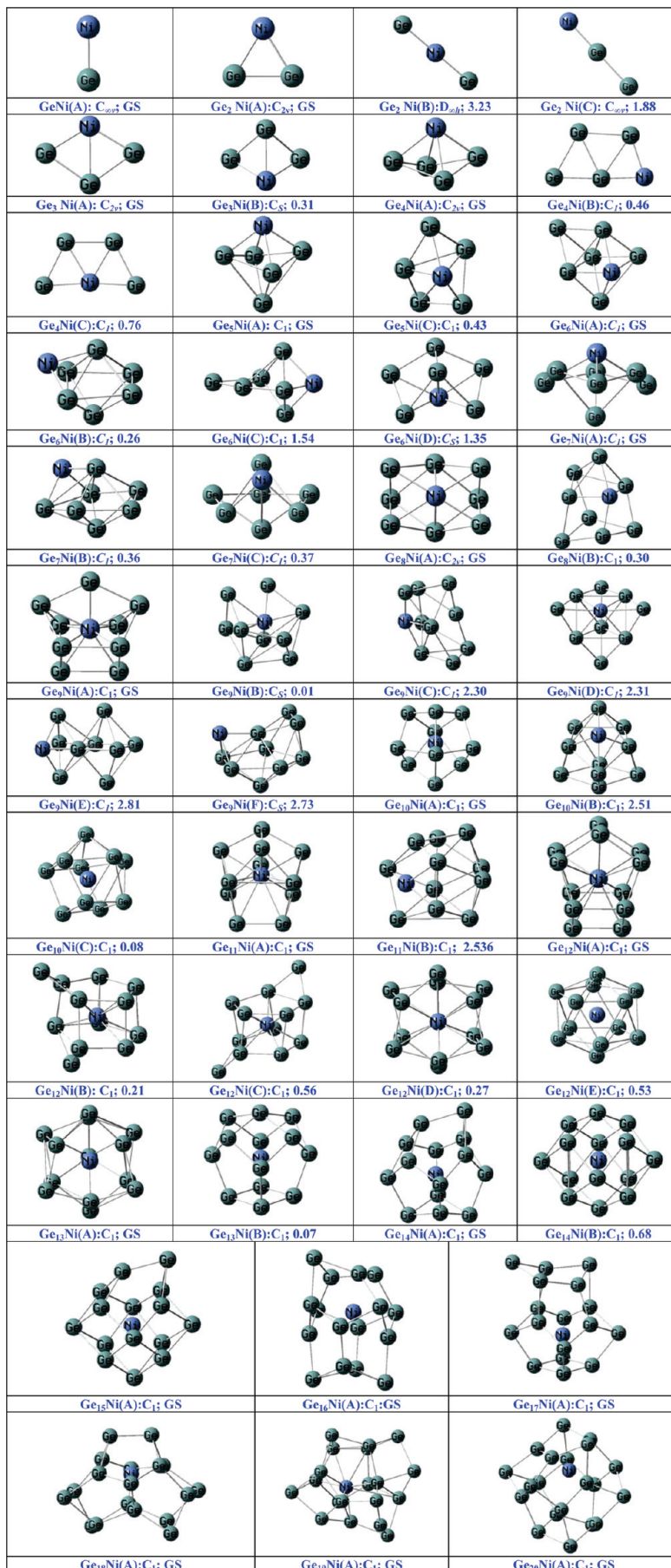


**Figure 2.** Optimized structures of Ge<sub>n</sub>Ni clusters with *n* = 2–20 with the point group symmetry and relative energies (in electronvolts) with respect to the GS isomer in each size.

of two pentagons and ten rhombi. The two pentagons share a common side and are also connected to six other rhombi. Both  $\text{Ge}_{14}\text{Ni}(\text{A})$  and  $\text{Ge}_{15}\text{Ni}(\text{A})$  can be taken as a “bag” kind of structure.

The structure  $\text{Ge}_{16}\text{Ni}(\text{A})$  has  $D_{4d}$  symmetry. It has two widely separated squares and eight pentagons. Each square is connected to four pentagons separately. This structure is not a symmetrical structure as found in a titanium-doped germanium cluster of the same size.<sup>49</sup> It is to be noted that with the increase of the size of the clusters beyond  $n = 13$ , the Ge cages start to distort, and this distortion continues up to the largest cluster in the present calculations. It is relevant to mention here that TM-doped  $\text{Ge}_n\text{H}_n$  clusters have very symmetric<sup>28</sup> structures. The H atoms saturate the dangling bonds on the Ge atoms leading to the stability of regular cages. This is similar to the case of Si cages. While it is well known that  $\text{Si}_{60}$  does not form a fullerene structure, unlike  $\text{C}_{60}$ , because of the unfavorable  $\text{sp}^2$  hybridization on the former, a  $\text{Si}_{60}\text{H}_{60}$  cluster forms a perfect icosahedral fullerene cage.<sup>25</sup> Presence of the H atoms not only saturates the dangling bonds on the Si atoms, but also leads to an  $\text{sp}^3$  hybridization on the Si atoms leading to the stability of the fullerene cage. Other bigger clusters ( $n > 16$ ) in the present study also show distorted structures. In summary, the growth behavior of a Ni-doped Ge clusters follow a definite trend. In smaller clusters, the nature changes from planar to a three-dimensional ground-state structure where the nickel atom absorbs exohedrally. This continues from  $n = 1$ –7. For  $n = 8$ , the Ni atom is partially enclosed by the Ge atoms in the ground-state structure  $\text{Ge}_8\text{Ni}(\text{A})$ . From  $n = 9$  onward, the Ni atom is adsorbed endohedrally and the clusters form cage-like structures. This continues up to  $n = 15$ . For bigger clusters, the nickel atoms stay inside the cluster, but the cage gets distorted.

**C. Electronic Structure of  $\text{Ge}_n\text{Ni}$  Clusters.** In this section we present our analysis of the electronic structure and relative stability of  $\text{Ge}_n\text{Ni}$  clusters of different sizes, i.e., different number of Ge atoms. For reasons mentioned earlier, we explore whether electron counting rules can explain the relative stability of Ni-doped Ge clusters. However, the WW rule is not crucial in explaining relative stabilities of these clusters because of a reason explained below.

To monitor relative stability of Ni-doped Ge clusters with increasing number of Ge atoms, we study their binding energy (BE), EE, the gap between the highest occupied and the lowest unoccupied molecular orbitals (HOMO–LUMO gap), and the second order energy difference ( $\Delta_2$ ). These quantities are defined as follows.

BE is defined as the energy gained in assembling a cluster from its isolated constituents

$$\text{BE} = \sum E_A - E_{\text{T}}(\text{cluster}) \quad (1)$$

$\sum E_A$  is the sum of the ground-state total energies of all the isolated atoms constituting a cluster, and  $E_{\text{T}}(\text{cluster})$  is the total energy of the cluster. EE is the energy gain in incorporating a Ni atom in the lowest energy isomer of the pure  $\text{Ge}_n$  cluster

$$\text{EE} = E_{\text{T}}(\text{Ge}_n) + E_{\text{T}}(\text{Ni}) - E_{\text{T}}(\text{Ge}_n\text{Ni}) \quad (2)$$

$E_{\text{T}}$ s are the total energies of the respective systems. It is in calculating EE that the WW rule<sup>35</sup> has to be enforced, as argued by Reveles and Khanna.<sup>34</sup> The ground states of all the  $\text{Ge}_n$  and  $\text{Ge}_n\text{Ni}$  clusters are singlets except  $n = 2$ , while the ground state of a Ni atom is a triplet. Therefore, taking ground-state total energies of all the clusters and atoms in eq 2, spin conservation

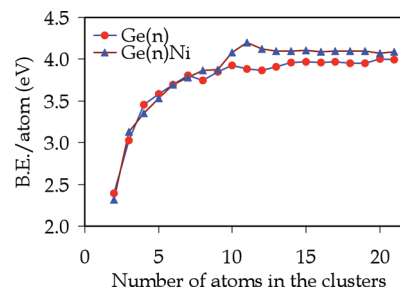


**Figure 3.** Variation of BE per atom of pure and Ni-doped germanium clusters as a function of size.

is not satisfied. On the other hand, it is easy to see that, if we consider the Ni atom in its singlet excited state, spin conservation is satisfied for all  $n \geq 2$ . However, note that taking the triplet ground-state energy of a Ni atom in eq 2 will only shift EEs for all  $n$  by an amount equal to the singlet–triplet splitting of the Ni atom and will not alter the nature of the EE vs  $n + 1$  curve. Therefore, we cannot comment whether it is necessary to include WW rules in order to explain the relative stabilities. For that we will need to study different TM-encapsulated  $\text{Ge}_n$  clusters. This will be the subject of a future work. While calculating EE of cationic clusters, one can consider two processes: adding a neutral Ni atom to a charged  $\text{Ge}_n$  cluster or adding a charged Ni atom to a neutral  $\text{Ge}_n$  cluster. The EEs in the two situations are given by

$$\text{EE} = E_{\text{T}}(^2\text{Ge}_n^+) + E_{\text{T}}(^1\text{Ni}) - E_{\text{T}}(^2\text{Ge}_n\text{Ni}^+) \quad (3a)$$

or

$$= E_{\text{T}}(^1\text{Ge}_n) + E_{\text{T}}(^2\text{Ni}^+) - E_{\text{T}}(^2\text{Ge}_n\text{Ni}^+) \quad (3b)$$

where we have used the fact that the ground states of  $\text{Ge}_n^+$  and  $\text{Ge}_n\text{Ni}^+$  clusters are doublets. We use the smaller of these two EEs at each size for our analysis. The second-order energy difference for  $\text{Ge}_n\text{Ni}$  clusters is defined as

$$\begin{aligned} \Delta_2(n) = \{E_{\text{T}}(\text{Ge}_{n+1}\text{Ni}) - E_{\text{T}}(\text{Ge}_n\text{Ni})\} - \{E_{\text{T}}(\text{Ge}_n\text{Ni}) - \\ E_{\text{T}}(\text{Ge}_{n-1}\text{Ni})\} = E_{\text{T}}(\text{Ge}_{n+1}\text{Ni}) + E_{\text{T}}(\text{Ge}_{n-1}\text{Ni}) - \\ 2E_{\text{T}}(\text{Ge}_n\text{Ni}) \quad (4) \end{aligned}$$

To calculate second-order energy differences for charged clusters, total energies of charged clusters have to be used in this equation.  $\Delta_2$  is a measure of the energy gain in formation of clusters of size  $n$  by cohesion of an atom to size  $n - 1$  or due to fragmentation of size  $n + 1$ . Peaks in this parameter, plotted as  $n$ , indicate more stable clusters.

BE per Ge atom for pure and Ni-doped Ge clusters are plotted in Figure 3. BE initially increases with cluster size but saturates to a limiting value beyond  $n \approx 13$ . Beyond  $n = 9$ , Ni doping increases BE indicating that Ni doping enhances thermodynamic stability of the Ge clusters. BE per atom shows peaks at  $n = 10$  for both pure and Ni-doped Ge clusters. (Please note that BE and all other quantities are plotted as a function of total number of atoms in the cluster.) Stability of  $\text{Ge}_{10}\text{Ni}$  is very interesting. If we assume that each Ge atom donates one electron to the valence manifold and since the Ni atom has 10 valence electrons then this size corresponds to a 20-electron cluster. The situation is similar to a



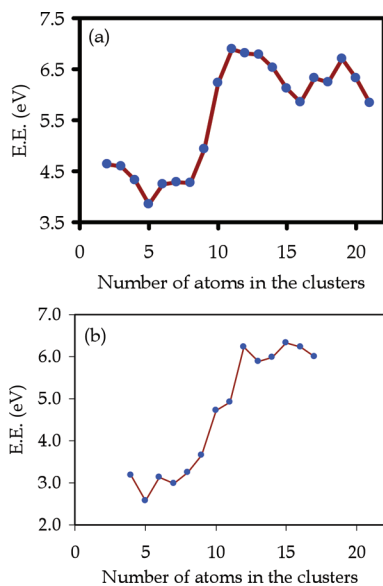


**Figure 4.** Variation of EE of Ge<sub>n</sub>Ni (a) neutral and (b) cation clusters with size.

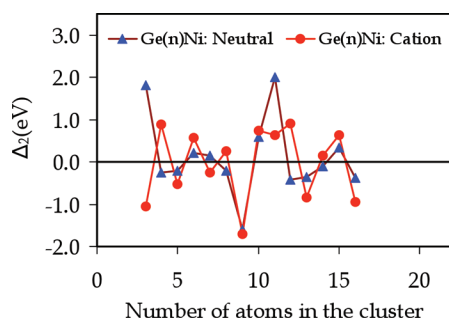


**Figure 5.** Variation of  $\Delta_2$  of Ge<sub>n</sub>Ni neutral and cation clusters with size.

Si<sub>12</sub>Fe cluster. However, there is no enhanced stability for Ge<sub>8</sub>Ni, which corresponds to an 18-electron cluster.

Variation of EE with size for both neutral and cationic Ge<sub>n</sub>Ni clusters is plotted in Figure 4. In the neutral clusters, EE has a peak at *n* = 10. Interestingly, in the cationic clusters, EE has a peak at *n* = 11. Thus both in the neutral and cationic series, 20-electron clusters have enhanced stability. A peak in EE indicates in which the Ge<sub>n</sub> cluster it is most favorable to incorporate a Ni atom. A related but slightly different question is which is the most stable cluster as successive Ge atoms are added. This is given by  $\Delta_2$ .  $\Delta_2$  as a function of total number of atoms in neutral and cationic Ge<sub>n</sub>Ni clusters is shown in Figure 5. Peaks in the neutral and cationic series occur at *n* = 10 and 11, respectively, again indicating enhanced stability of 20-electron clusters.

While the above parameters indicate thermodynamic stability of a cluster, kinetic stability of clusters in chemical reactions is indicated by HOMO–LUMO gaps. The larger the gap, the less reactive a cluster is. HOMO–LUMO gaps of neutral and Ge<sub>n</sub> and Ge<sub>n</sub>Ni clusters are plotted in Figure 6. It readily becomes obvious that all these clusters have large HOMO–LUMO gaps in excess of 1 eV for all sizes. Overall, there is a decrease of the gap with size in both pure and Ni-doped clusters. However, there are some local oscillations over and above the decreasing trend. Although there is no sharp global peak as in other quantities, there is a clear local peak at *n* = 10 in the Ge<sub>n</sub>Ni series. This again points to an enhanced stability of 20-electron clusters. It is also worth noticing that at most sizes there is a decrease in the HOMO–LUMO gap on Ni encapsulation. The drops are quite marked at *n* = 5, 6, 14, 15, and 17. In contrast to this general trend, the gap rises at *n* = 8, 11, 13, and 19.

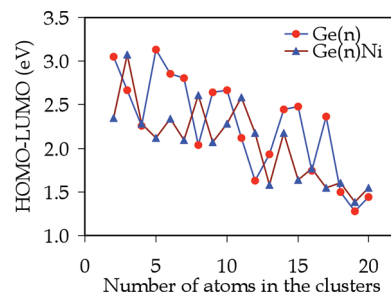


**Figure 6.** Variation of HOMO–LUMO of Ge<sub>n</sub> and Ge<sub>n</sub>Ni clusters with size.

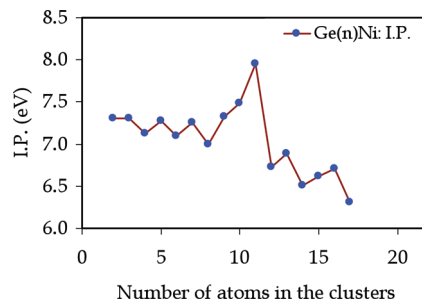


**Figure 7.** Variation of IP of the Ge<sub>n</sub>Ni clusters with size.

As mentioned earlier, enhanced stability of 20-electron clusters can be rationalized in terms of electronic shell models developed for metal clusters. It has been shown for metal clusters that whenever a new shell starts getting occupied for the first time, the adiabatic ionization potential (IP) drops sharply. For example, because *n* = 20 is a filled shell configuration for Li<sub>n</sub> clusters, there is a sharp drop in IP from *n* = 20 to 21.<sup>36</sup> If the enhanced stability of the 20-electron Ge<sub>10</sub>Ni cluster is due to a filled shell configuration then there should be a sharp drop in IP as the next Ge atom is added. This is precisely what we see in the IP values of these clusters, as plotted in Figure 7. There is a peak in IP at *n* = 10 and a sharp drop at *n* = 11. In fact, the IP drops from 7.95 eV for *n* = 10 to 6.73 eV. Sharp drop in IP from *n* = 10–11 is perhaps the strongest indication that assumption of a nearly free-electron gas inside the Ge cage is a good model for Ge<sub>n</sub>Ni clusters, similar to Si<sub>n</sub>TM clusters.<sup>34</sup> That a nearly free-electron gas is a better description than octet rule on the central Ni atom is also indicated by Mulliken population analysis for these systems. The Mulliken charge on the Ni atom encapsulated in a Ge cage (*n* > 8) varies between −1.3 (for *n* = 20) and −2.7 (for *n* = 10), indicating that a picture of each Ge atom donating one electron is not correct. In the Si<sub>12</sub>Cr cluster also, the Mulliken charge on the central Cr atom is −1.1.<sup>56</sup>

Thus all measures of stability indicate that Ge<sub>n</sub>Ni clusters obey the electron-counting rule of the shell model to the extent that 20-electron clusters have enhanced stability. A Ni atom itself having 10 valence electrons, whether an 8-electron Ge<sub>n</sub>TM cluster has enhanced stability cannot obviously be tested. This question may, however, be addressed with other TM atoms. Why 18-electron clusters do not show enhanced stability is a legitimate but difficult question to answer. We would only like to mention that the exact shell filling numbers depend on the model used. While the model of free electrons inside a sphere produces both 18 and 20 as shell filling numbers, free electrons moving in an isotropic 3D harmonic oscillator potential only have 20 as shell filling number.<sup>36</sup>

In any case, enhanced stability of 20-electron Ge<sub>n</sub>Ni clusters is an interesting result in view of the fact that controversies



regarding validity of electron-counting rules have not been completely resolved for  $\text{Si}_n\text{TM}$  clusters. Particularly interesting is the drop in IP for the 21-electron cluster  $\text{Ge}_{11}\text{Ni}$ . The IP of a  $\text{Ge}_{11}\text{Ni}$  cluster is in the same range as that of the TM atoms. Hence, it may be possible to form stable halide compounds of this cluster. Identification of such clusters can help identify new semiconductor-based “superatoms” that can be building blocks for cluster-assembled designer materials.

## Conclusions

In summary, a report on the study of geometry and electronic properties of neutral and cationic pure and Ni-doped  $\text{Ge}_n$  ( $n = 1-20$ ) clusters within DFT is presented. On the basis of the results, the following conclusions can be drawn. It is favorable to attach a Ni atom to Ge clusters at all sizes, as the EE turns out to be positive in every case. Clusters containing more than 8 Ge atoms are able to absorb Ni atom endohedrally in a Ge cage. In all Ni-doped clusters beyond  $n = 2$ , the spin on the Ni atom is quenched. More interesting is the relative stability of these clusters. As measured by their BE, EE, and  $\Delta_2$ , both neutral and cationic clusters having 20 valence electrons show enhanced stability, in agreement with shell model predictions. This also shows up in the IP values of the  $\text{Ge}_n\text{Ni}$  clusters, as there is a sharp drop in IP from  $n = 10$  to 11. Validity of nearly free-electron shell model is similar to that in  $\text{Si}_n\text{TM}$  clusters. While  $\text{Ge}_{10}\text{Ni}$  is a particularly stable species,  $\text{Ge}_{11}\text{Ni}$  with its smaller IP may form ionic compounds with halogen atoms. Although the signature of stability is not so sharp in the HOMO–LUMO gaps of these clusters, there is still a local maximum at  $n = 10$  for the neutral clusters, indicating enhanced stability of a 20-electron cluster. Identification of the stable species, and variation of chemical properties with size in the TM-doped Ge clusters will help design Ge-based superatoms. The present work is the first step in this direction, and it will be followed by more detailed studies on these systems.

**Acknowledgment.** Gaussian 03 calculations were performed on the cluster computing facility at HRI (<http://cluster.hri.res.in>).

## References and Notes

- Ho, K. M.; Shvartzburg, A. A.; Pan, B.; Lu, Z. Y.; Wang, C. Z.; Wacker, J. G.; Fye, J.; Jarrold, M. F. *Nature* **1998**, *392*, 582.
- Lokibe, K.; Tachikawa, H.; Azumi, K. *J. Phys. B: At. Mol. Opt. Phys.* **2007**, *40*, 427.
- Shvartzburg, A. A.; Jarrold, M. F. *Phys. Rev. A* **1999**, *60*, 1235.
- Jarrold, M. F.; Constant, V. A. *Phys. Rev. Lett.* **1991**, *67*, 2994.
- Benedict, L. X.; Puzer, A.; Williamson, A. J.; Grossman, J. C.; Galli, G.; Klepeis, J. E.; Raty, J. Y.; Pankratov, O. *Phys. Rev. B* **2003**, *68*, 85310.
- Brown, W. L.; Freeman, R. R.; Raghavachari, K.; Schluter, M. *Science* **1987**, *235*, 860.
- Hiura, H.; Miyazaki, T.; Kanayama, T. *Phys. Rev. Lett.* **2001**, *86*, 1733.
- Hayashi, S.; Kanzaya, Y.; Kataoka, M.; Nagarede, T.; Yamamoto, K. Z. *Phys. D: At. Mol. Clusters* **1993**, *26*, 144.
- Zhang, X.; Li, G.; Gao, Z. *Rapid Commun. Mass Spectrom* **2001**, *15*, 1573.
- Archibong, D. F.; St-Amant, A. *J. Chem. Phys.* **1998**, *109*, 962.
- Wang, J.; Wang, G.; Zhao, J. *Phys. Rev. B* **2001**, *64*, 205411.
- Zhao, C.; Balasubramanian, J. *Chem. Phys.* **2001**, *115*, 3121, and references therein.
- Wang, J.; Zhao, J.; Ding, F.; Shen, W.; Lee, H.; Wang, G. *Sol. State Comm.* **2001**, *117*, 593.
- Kikuchi, E.; Ishii, S.; Ohno, K. *Phys. Rev. B* **2006**, *74*, 195410.
- Ma, S.; Wang, G. *J. Mol. Struct.* **2006**, *767*, 75.
- Neukermans, S.; Wang, X.; Veldeman, N.; Janssens, E.; Silverans, R. E.; Lievens, P. *Int. J. Mass Spectrom.* **2006**, *252*, 145.
- Wang, J.; Han, J.-G. *J. Phys. Chem. B* **2006**, *110*, 7820.
- Jarrold, M. F.; Bower, J. E. *J. Chem. Phys.* **1992**, *96*, 9180.
- Rothlisberger, U.; Andreoni, W.; Parrinello, M. *Phys. Rev. Lett.* **1994**, *72*, 665.
- Kaxiras, E.; Jackson, K. *Phys. Rev. Lett.* **1993**, *71*, 727.
- Ho, K.-M.; Shvartzburg, A. A.; Pan, B.; Lu, Z.-Y.; Wang, C.-Z.; Wacker, J. G.; Fye, J.; Jarrold, M. F. *Nature (London)* **1998**, *392*, 582.
- Kumar, V.; Kawazoe, Y. *Phys. Rev. Lett.* **2001**, *87*, 045503.
- Kumar, V.; Kawazoe, Y. *Phys. Rev. Lett.* **2002**, *88*, 235504.
- Zdetsis, A. D. *Phys. Rev. B* **2007**, *76*, 075402.
- Barman, S.; Sen, P.; Das, G. P. *J. Phys. Chem. C* **2008**, *112*, 19963.
- Wang, L.; Li, D.; Yang, D. *Mol. Simulations* **2006**, *32*, 663.
- Zhang, D.; Ma, C.; Lin, C. *J. Phys. Chem. C* **2007**, *111*, 17099.
- Kumar, V.; Kawazoe, Y. *Phys. Rev. B* **2007**, *75*, 155425.
- Goicoechea, J. M.; Sevov, S. C. *J. Chem. Soc. Am.* **2006**, *128*, 4155.
- Wang, J.-Q.; Stegmaier, S.; Fässler, T. F. *Angew. Chem. Int. Ed.* **2009**, *48*, 1998.
- Huheey, J. E.; Keiter, E. A.; Keiter, R. L., *Inorganic Chemistry: principles of structure and reactivity*, 4th ed. (2000), New York: Harper-Collins College Publisher.
- Sen, Prasenjit; Mitas, Lubos *Phys. Rev. B* **2003**, *68*, 155404.
- Ling-ju, Guo; Gao-feng, Zhao; Yu-zong, Gu; Xia, Liu; Zhi, Zeng *Phys. Rev. B* **2008**, *77*, 195417.
- Reveles, J. U.; Khanna, S. N. *Phys. Rev. B* **2005**, *72*, 165413.
- Wigner, E.; Witmer, E. E. *Z. Phys.* **1928**, *51*, 859.
- de Heer, W. A. *Rev. Mod. Phys.* **1993**, *65*, 611.
- Koyasu, K.; Akutsu, M.; Mitsui, M.; Nakajima, A. *J. Am. Chem. Soc.* **2005**, *127*, 4998.
- Khanna, S. N.; Castleman, A. W., Jr. *J. Phys. Chem. C* **2009**, *113*, 2664.
- Kiichirou, Koyasu; Junko, Atobe; Minoru, Akutsu; Masaaki, Mitsui; Atsushi, Nakajima *J. Phys. Chem. A* **2007**, *111* (1), 42.
- Burke, K.; Perdew, J. P.; Wang, Y., in *Electronic Density Functional Theory: Recent Progress and New Directions*, Ed. Dobson, J. F.; Vignale, G. Das, M. P., Plenum, 1998.
- Perdew, J. P., in *Electronic Structure of solids '91*, Ed. Ziesche, P. Eschrig, H., Akademie Verlag, Berlin, 1991.
- Becke, A. D. *Phys. Rev. A* **1988**, *38*, 3098.
- Lee, C.; Yang, W.; Parr, R. G. *Phys. Rev. B* **1988**, *27*, 785.
- Shim, I.; Sai Baba, M.; Ginerich, K. *Chem. Phys.* **2002**, *277*, 9.
- (a) Frisch, M. J.; Trucks, G. W.; Schlegel, H. B.; Scuseria, G. E.; Robb, M. A.; Cheeseman, J. R.; Zakrzewski, V. G.; Montgomery, J. A., Jr.; Stratmann, R. E.; Burant, J. C.; Dapprich, S.; Millam, J. M.; Daniels, A. D.; Kudin, K. N.; Strain, M. C.; Farkas, O.; Tomasi, J.; Barone, V.; Cossi, M.; Cammi, R.; Mennucci, B.; Pomelli, C.; Adamo, C.; Clifford, S.; Ochterski, J.; Petersson, G. A.; Ayala, P. Y.; Cui, Q.; Morokuma, K.; Malick, D. K.; Rabuck, A. D.; Raghavachari, K.; Foresman, J. B.; Cioslowski, J.; Ortiz, J. V.; Baboul, A. G.; Stefanov, B. B.; Liu, G.; Liashenko, A.; Piskorz, P.; Komaromi, I.; Gomperts, R.; Martin, R. L.; Fox, D. J.; Keith, T.; Al-Laham, M. A.; Peng, C. Y.; Nanayakkara, A.; Challacombe, M.; Gill, P. M. W.; Johnson, B.; Chen, W.; Wong, M. W.; Andres, J. L.; Gonzalez, C.; Head-Gordon, M.; Replogle, E. S.; Pople, J. A. *Gaussian 98*, Revision A.9; Gaussian, Inc.: Pittsburgh, PA, 1998. (b) Frisch, M. J.; Trucks, G. W.; Schlegel, H. B.; Scuseria, G. E.; Robb, M. A.; Cheeseman, J. R.; Montgomery, J. A., Jr.; Vreven, T.; Kudin, K. N.; Burant, J. C.; Millam, J. M.; Iyengar, S. S.; Tomasi, J.; Barone, V.; Mennucci, B.; Cossi, M.; Scalmani, G.; Rega, N.; Petersson, G. A.; Nakatsuji, H.; Hada, M.; Ehara, M.; Toyota, K.; Fukuda, R.; Hasegawa, J.; Ishida, M.; Nakajima, T.; Honda, Y.; Kitao, O.; Nakai, H.; Klene, M.; Li, X.; Knox, J. E.; Hratchian, H. P.; Cross, J. B.; Bakken, V.; Adamo, C.; Jaramillo, J.; Gomperts, R.; Stratmann, R. E.; Yazyev, O.; Austin, A. J.; Cammi, R.; Pomelli, C.; Ochterski, J. W.; Ayala, P. Y.; Morokuma, K.; Voth, G. A.; Salvador, P.; Dannenberg, J. J.; Zakrzewski, V. G.; Dapprich, S.; Daniels, A. D.; Strain, M. C.; Farkas, O.; Malick, D. K.; Rabuck, A. D.; Raghavachari, K.; Foresman, J. B.; Ortiz, J. V.; Cui, Q.; Baboul, A. G.; Clifford, S.; Cioslowski, J.; Stefanov, B. B.; Liu, G.; Liashenko, A.; Piskorz, P.; Komaromi, I.; Martin, R. L.; Fox, D. J.; Keith, T.; Al-Laham, M. A.; Peng, C. Y.; Nanayakkara, A.; Challacombe, M.; Gill, P. M. W.; Johnson, B.; Chen, W.; Wong, M. W.; Gonzalez, C.; Pople, J. A. *Gaussian 03*, Revision D.1; Gaussian, Inc.: Wallingford, CT, 2005.
- Ling-Ju, Guo; Xia, Liu; Gao-Feng, Zhao; You-Hua, Luo *J. Chem. Phys.* **2007**, *126*, 234704.
- Lubos, Mitas; Grossman, Jeffrey C.; Stich, Ivan; Tobik, Jaroslav *Phys. Rev. Lett.* **2000**, *4* (7), 1979.
- Moran, D.; Woodcock, H. L.; Chen, Z.; Schaefer III, H. F.; Schleyer, P. v. R. *J. Am. Chem. Soc.* **2003**, *125*, 11442.
- Bandyopadhyay, Debashis *J. Appl. Phys.* **2008**, *104*, 084308.
- Kawamura, H.; Kumar, V.; Kawazoe, Y. *Phys. Rev. B* **2005**, *71*, 075423.
- Kumar, V.; Kawazoe, Y. *Phys. Rev. B* **2002**, *65*, 073404.
- Kawamura, H.; Kumar, V.; Kawazoe, Y. *Phys. Rev. B* **2004**, *70*, 245433.
- Kumar, V.; Kawazoe, Y. *Appl. Phys. Lett.* **2003**, *83*, 2677.
- Broer, R.; Aissing, G.; Nieuwpoort, W. C. *International Journal of Quantum Chemistry: Quantum Chemistry Symposium* **1988**, *22*, 297.
- Lu, J.; Nagase, S. *Chem. Phys. Lett.* **2003**, *372*, 394.
- Reveles, J. U.; Khanna, S. N. (Private communication).